

Scanning electrochemical microscopy as an etching tool for ITO patterning

Dr. Federico Grisotto¹, Dr. Romain Metaye¹, Dr. Bruno Joussetme¹, Dr. Bernard Geffroy^{1,2}, Dr. Serge Palacin¹ and Dr. Julienne Charlier¹

[1] CEA-Saclay, DSM/IRAMIS/SPCSI/ Laboratory of Chemistry of Surfaces and Interfaces, 91191 Gif-sur-Yvette Cedex, France., [2] CEA/Ecole Polytechnique, LPICM, F-91128, Palaiseau, France

Supplementary information

A/ Preparation and characterization of microdisk electrodes.

The Pt microdisk electrodes are prepared according to the literature. Briefly, the end of a glass capillary is sealed such that a conical shape is obtained. A straight 100, 50, 25, or 10 μm diameter Pt wire (99.9% purity, Goodfellow, United Kingdom) is then positioned at the bottom of the sealed borosilicate glass capillary. The capillary is then slowly sealed onto the wire using a heated resistor coil. The sealed wire is then electrically connected to a larger wire by welding with tin. The microdisk electrode is then polished using sandpaper by gradually increasing grit size (600 and 1200) such that the RG value (RG = ratio of glass to metallic radii) falls if possible under 10 and a smooth surface is obtained (fig. Ea). Before use, UMEs are washed under sonication in Milli-Q water. The quality of the microdisk electrode is checked by recording the steady-state voltammogram of a well-characterized systems having rapid heterogeneous electron transfer ($\text{Fe}(\text{CN})_6^{3-}/\text{Fe}(\text{CN})_6^{4-}$). The initial potential is set from -0.25 vs. Ag wire to 0.4 V, and reversed and the current sensitivity to 100 nA. The UMEs are considered as satisfactory if the reverse scan retraces the forward scan (fig. Eb).

The tip is moved by a horizontal and vertical translation stage driven by an electric micro-step engine. Potential and current are imposed or measured by a potentiostat/galvanostat system integrated to the SECM370 workstation. The z-approach curves and the X-Y planarity of the sample are realized by setting the microelectrode potential on the reduction plateau of $\text{Fe}(\text{CN})_6^{3-}$ (5×10^{-3} mol. dm^{-3} , KCl 0.1 mol. dm^{-3}). The current as a function of time is recorded upon approaching the surface and translated later into a current-distance curve using the SECM calibration curves for insulating and conducting substrates and the approach

speed.^[7, 8] Both in the negative feedback and in the positive feedback, the magnitude of the variation of the current fits the theoretical treatment (fig.Ec).

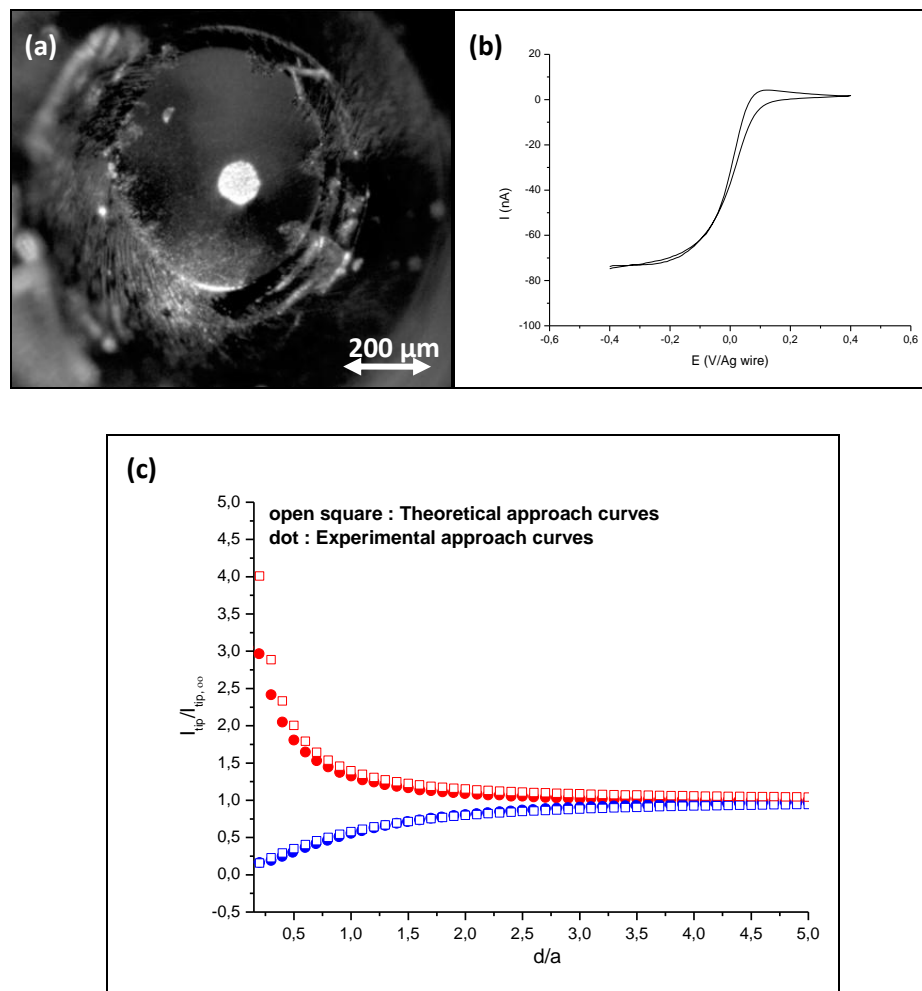


Figure A: (a) optical microscopy image of the 100µm-Pt UME ($RG = 4.9$), (b) steady-state current at the 100 µm-Pt UME, (c) experimental vs. theoretical approach curves for a conducting substrate (red), and an insulating substrate (blue).

B/ OLEDs fabrication.

The OLED devices consisting of multiple organic layers were fabricated on pre-patterned ITO coated PET substrates. The device structure was PET/ITO/CuPc (10nm)/ α -NPB (50 nm)/Alq₃ (60 nm)/LiF (1.2 nm)/Al (100nm). Copper (II) phthalocyanine (CuPc), 4, 4'-bis[N-(1-naphtyl)-N-phenylamino]biphenyl (α -NPB), aluminium tris(8-quinolinolato) (Alq₃) were used as a hole injection, hole transport and electron transport layers respectively. As a cathode, lithium fluoride (LiF) and aluminium (Al) were used to improve electron injection.

All the layers were evaporated at a deposition rate of 0.2 nm/s without breaking high vacuum ($\sim 10^{-7}$ mbar).

C/ Redox couples in the water discharge region.

Table A. standard potential of several redox couples in the water discharge region^[1]

Oxidation reaction	$E^\circ/\text{V vs. SHE}$
$\text{H}_2\text{O} \rightarrow \text{HO}^\cdot + \text{H}^+ + \text{e}^-$	2.80
$\text{O}_{2(g)} + \text{H}_2\text{O} \rightarrow \text{O}_{3(g)} + 2 \text{H}^+ + 2\text{e}^-$	2.08
$2 \text{H}_2\text{O} \rightarrow \text{H}_2\text{O}_2 + 2 \text{H}^+ + 2\text{e}^-$	1.77
$\text{H}_2\text{O}_2 \rightarrow \text{HO}_2^\cdot + \text{H}^+ + \text{e}^-$	1.44

D/ Currents recorded simultaneously at the tip and on the substrate in a four-electrochemical cell configuration.

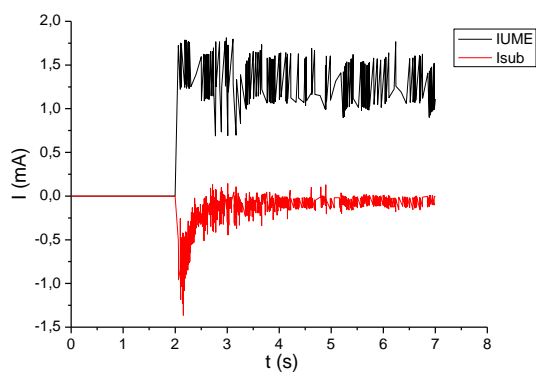


Figure B: simultaneously recorded currents at the UME (black) and at the ITO substrate (red) when the UME is biased at 10 V vs. Ag wire and the ITO substrate at -0.4 V vs. Ag wire. $[\text{AA}] = 2 \text{ mol.dm}^{-3}$, $[\text{H}_2\text{SO}_4] = 0.25 \text{ mol.dm}^{-3}$, 100 μm -Pt UME, working distance = 20 μm , $t = 5 \text{ s}$.

E/ Influence of the working distance on the width of the etched pattern.

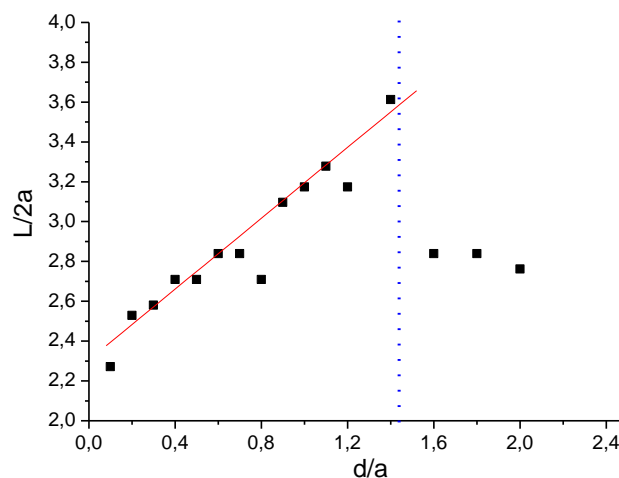


Figure C: Width of the etched dots as a function of the normalized working distance (ratio between the working distance, d , and the tip's radius, a). chronoamperometry, $100\ \mu\text{m}$ -Pt UME, $E_{\text{UME}} = 7\ \text{V}$ vs. Ag wire, $E_{\text{sub}} = -0.2\ \text{V}$ vs. Ag wire, $t=5\ \text{s}$, $[\text{AA}]=2\ \text{mol}\cdot\text{dm}^{-3}$, $[\text{H}_2\text{SO}_4]=0.25\ \text{mol}\cdot\text{dm}^{-3}$. Red solid line: linear fit; blue dashed line: limit between complete and incomplete etching process.

F/ Etching process on ITO/PET flexible substrate

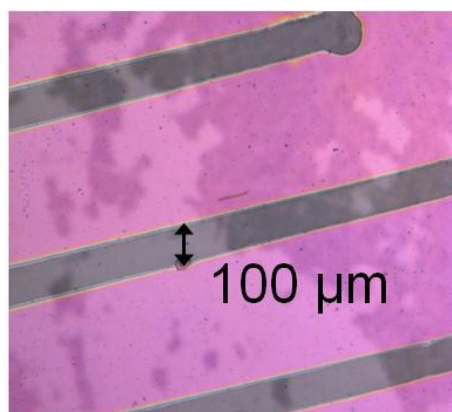


Figure D: Optical image of etched ITO deposited on PET. $25\ \mu\text{m}$ -Pt UME, working distance = $10\ \mu\text{m}$, $v=100\ \mu\text{m}\cdot\text{s}^{-1}$, $[\text{AA}]=2\ \text{mol}\cdot\text{dm}^{-3}$. (no sulfuric acid)

G/ Etching of modified ITO substrates.

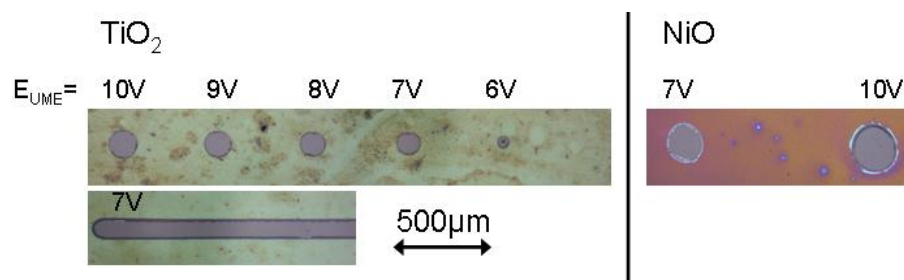


Figure E: Optical images of etched dots on ITO/ TiO_2 and ITO/ NiO bilayers for different E_{UME} . $E_{\text{sub}} = -0.4 \text{ V}$ vs. Ag wire, $50 \mu\text{m}$ -Pt UME, working distance = $10 \mu\text{m}$, $t=5\text{s}$, $[\text{AA}]=2\text{mol.dm}^{-3}$

[1] E. Brillas, I. Sires and M. A. Oturan, *Chem. Rev.* **2009**, *109*, 6571.